Attachment 4

REPORT NO. 82-32

DRF 137-0010

AUGUST 1982

STRUCTURAL ANALYSIS OF PEACH BOTTOM 2/3 REACTOR PRESSURE VESSEL HEAD DROP, SHROUD HEAD ASSEMBLY DROP, AND STEAM DRYER ASSEMBLY DROP CONDITIONS

PREPARED BY: M.L. HERRERA — DATE 8/23/82

G. MOK — DATE 8/23/82

REVIEWED BY: H.S. MEHTA — DATE 8/23/82

APPROVED BY: S. RANGANATH — DATE 8/23/82

O. OATES — DATE 9/3/82

NUCLEAR POWER SYSTEMS ENGINEERING DEPARTMENT

GENERAL ELECTRIC COMPANY, SAN JOSE, CALIFORNIA

TABLE OF CONTENTS

Summary

A detailed finite element elastic-plastic analysis was performed to evaluate the effects of the vessel head drop, shroud head drop and steam dryer assembly drop for the Peach Bottom 2/3 plants. The results of the analysis show that structural integrity of the vessel and shroud is maintained, although some yielding does occur in the vessel flange region.

Further, no damage to the fuel is predicted since the component geometry precludes damage to the fuel. In view of the fact that there is no significant damage to the reactor components or the fuel, no release of radioactivity is expected as a result of the drop.

1.0 INTRODUCTION

The purpose of this analysis is to evaluate the structural consequences of dropping the Peach Bottom 2/3 reactor pressure vessel head, steam dryer, and steam separator (shroud head assembly) during maintenance operations. The vessel head was assumed to be dropped resulting in impact on the reactor vessel flange. It is conservatively assumed that the head rotates 90° during the drop, producing local point impact between the vessel flange and the head. The shroud head and dryer were assumed to drop from a height sufficient to generate the steady state velocity of the two assemblies as they move through water and are under the action of the fluid drag forces. In reality the dryer assembly impacts the shroud head assembly. However, it is conservative to assume the impact with the main body of the shroud since no credit is taken for energy absorbed by the shroud head assembly.

An elastic-plastic dynamic analysis was performed for both the vessel head drop and shroud head drop. Stress and displacements following impact were plotted. The results show that the structural integrity of the vessel and shroud are maintained and therefore there will not be any significant release of radioactivity.

2.0 VESSEL HEAD DROP

A finite element analysis was performed to determine the vessel response when impacted by the vessel head. The ANSYS computer code (Ref. 1) was used for the analysis. Due to symmetry, only a 180° segment of the vessel body between the vessel-head flange and the bottom of the support skirt was modelled. The plane stress isoparametric quadrilateral element from the ANSYS element library was used to model the reactor vessel body. The model reflects the longitudinal and lateral, extensional and inextensional effects. Transverse effects are considered negligible and therefore the use of the plane stress option is justified. The model contains 43 nodes and 31 elements. To simulate the impact of the vessel head with the vessel, the ANSYS gap element was used. Figure 1 shows the modelling of the vessel and vessel head used in the analysis. The bottom row of elements represents the reactor vessel skirt. Nodes 6 and 43 define the gap element.

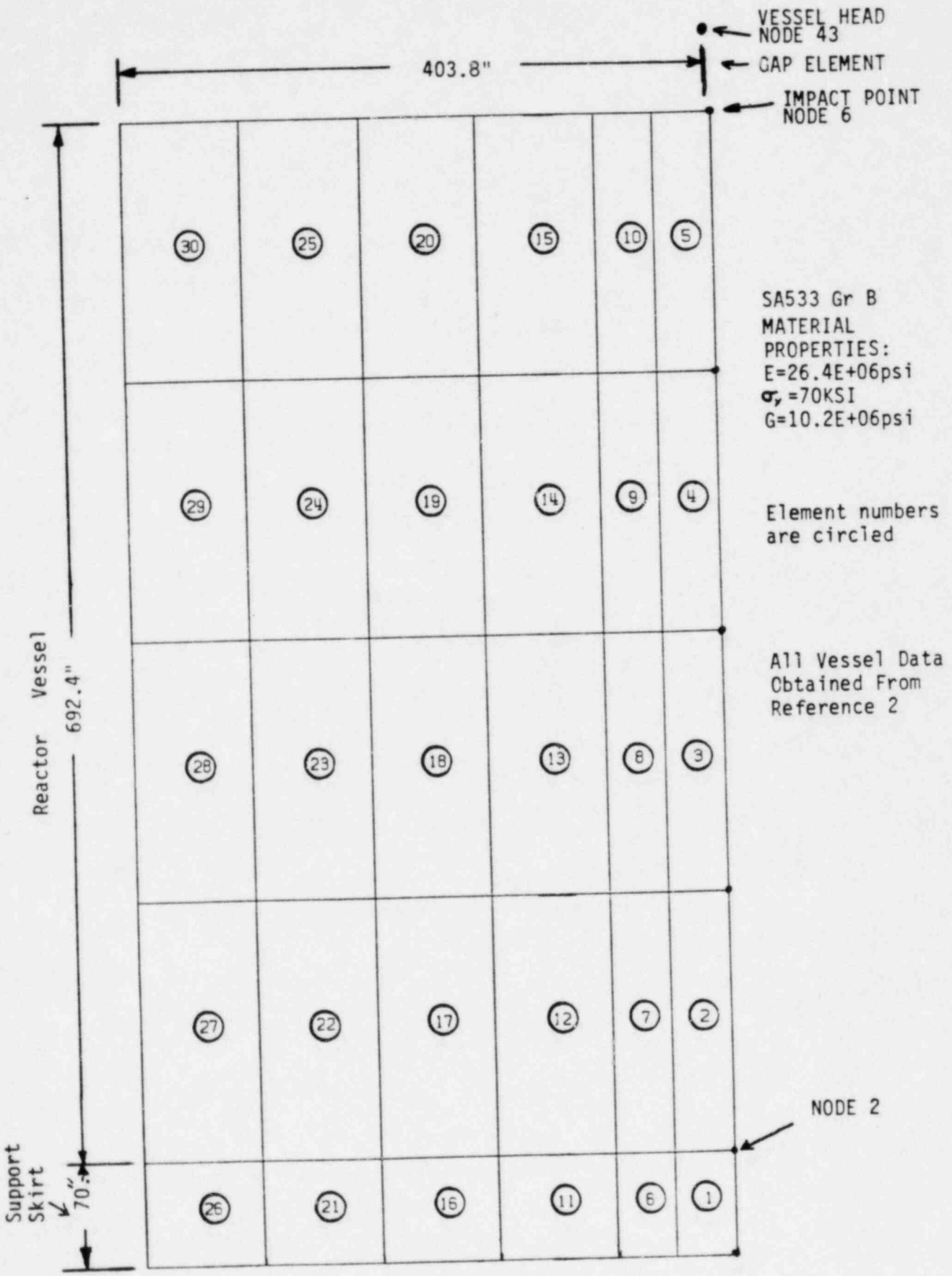

FIGURE 1 Vessel finite Element Model

2.1 Mass And Velocity Of Falling Head

The actual height of drop for the vessel head was specified as 24 feet (Ref. 3). The weight of the head is 96 tons and the weight of the strongback and crane hook is approximately 20 tons. Since the information of the drop height and the weight of the strongback was not available at the time the analysis was performed, it was assumed that the drop height was 40 ft. and the drop weight was 96 tons (Figure 2). This is conservative since the total energy of impact as analyzed, is 96 (2000)(40) = 7.68 X 10^6 ft-lb. The actual impact energy in a postulated drop is (96 +20) (2000) (24) = 5.568 X 10^6 ft-lb. The results of the analysis presented here are conservative and can be used to evaluate the structural consequences of the vessel head drop.

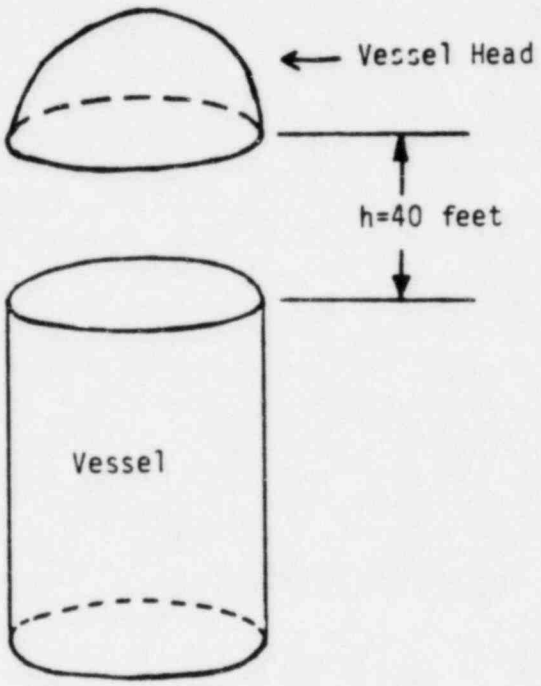

Figure 2 Drop Height

The impacting mass is: $M = 96(2000)/386.4 = 496.9$ lbf-sec/in^2

Since only one half of the vessel is being modelled due to symmetry, a value of M/2 is used in the analysis.

The effective travel, assuming that the head rotates 90^o such that a point impact occurs is h=480" - 139.625" = 340.4". Figure 3 shows the impact configuration.

The velocity at impact is :

$$V_o = \sqrt{2gh} = \sqrt{2(386.4)(340.4")}$$

$$V_o = 512.9 \text{ in/sec}$$

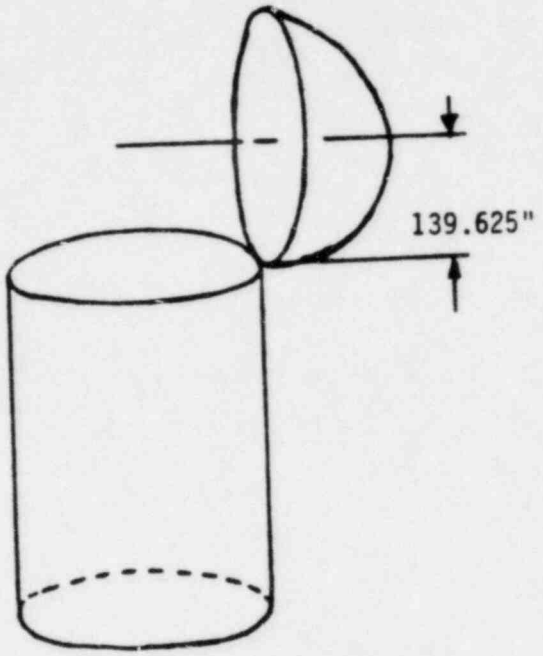

Figure 3 Impact Configuration

In simulating the head drop, node 43 of the finite element model is given a velocity of 512.9 in/sec just before closure of the gap. At the same time node 43 is subjected to a downward force equivalent to its weight.

The material behavior is taken to be perfecty plastic with a yield strength of 70 Ksi (Reference 4).

2.2 Vessel Head Drop Results

Figures 4 and 5 show the axial stress at elements 1 and 5, and deflections at nodes 2 and 6 respectively (See Figure 1). The wave propagation, is clearly evident from the figures takes approximately .003 seconds to reach the top of the support skirt. The maximum deflection at the point of impact and top of the support skirt is 1.65 and .35 inches respectively.

Yielding occurs rapidly at element 5 which is the location of impact. Yielding occurs in the support skirt .077 seconds into the transient. The yielding in the support skirt indicates that buckling should be considered.

The results of the finite element analysis indicate extensive inelastic yielding in the immediate element at the point of impact, and throughout the reactor support skirt. Subsequent analyses with a more refined model confirmed that the yielding in the region of impact is localized.

A more detailed analysis (Appendix A) was performed to determine if buckling occurs, taking into consideration dispersion of the travelling wave at the vessel-skirt junction, and reflection of waves at the skirt-foundation junction. The analysis confirms that buckling of the support skirt will not occur as a result of the impact.

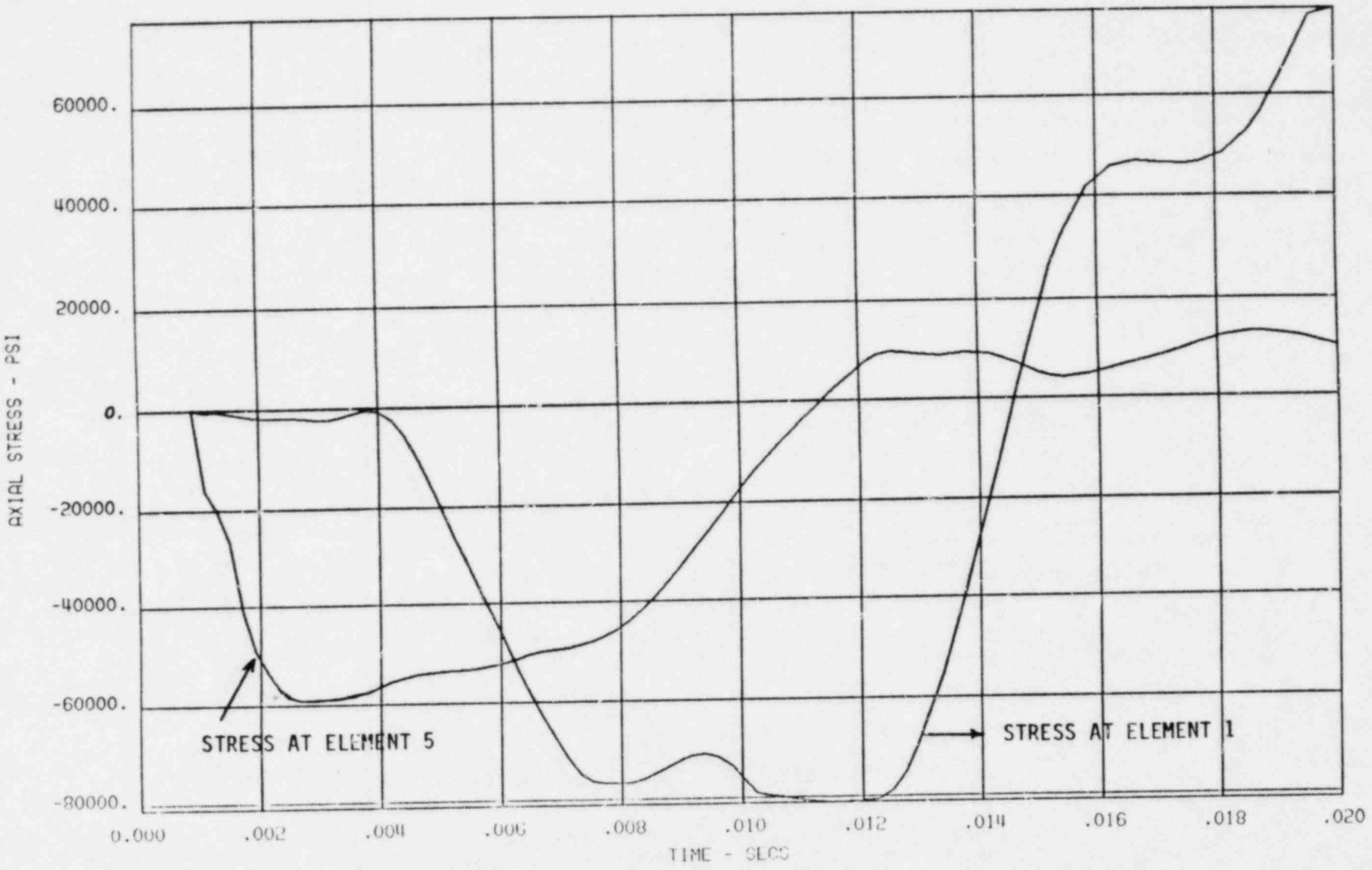

FIGURE 4 AXIAL STRESS AT ELEMENTS 1 AND 5

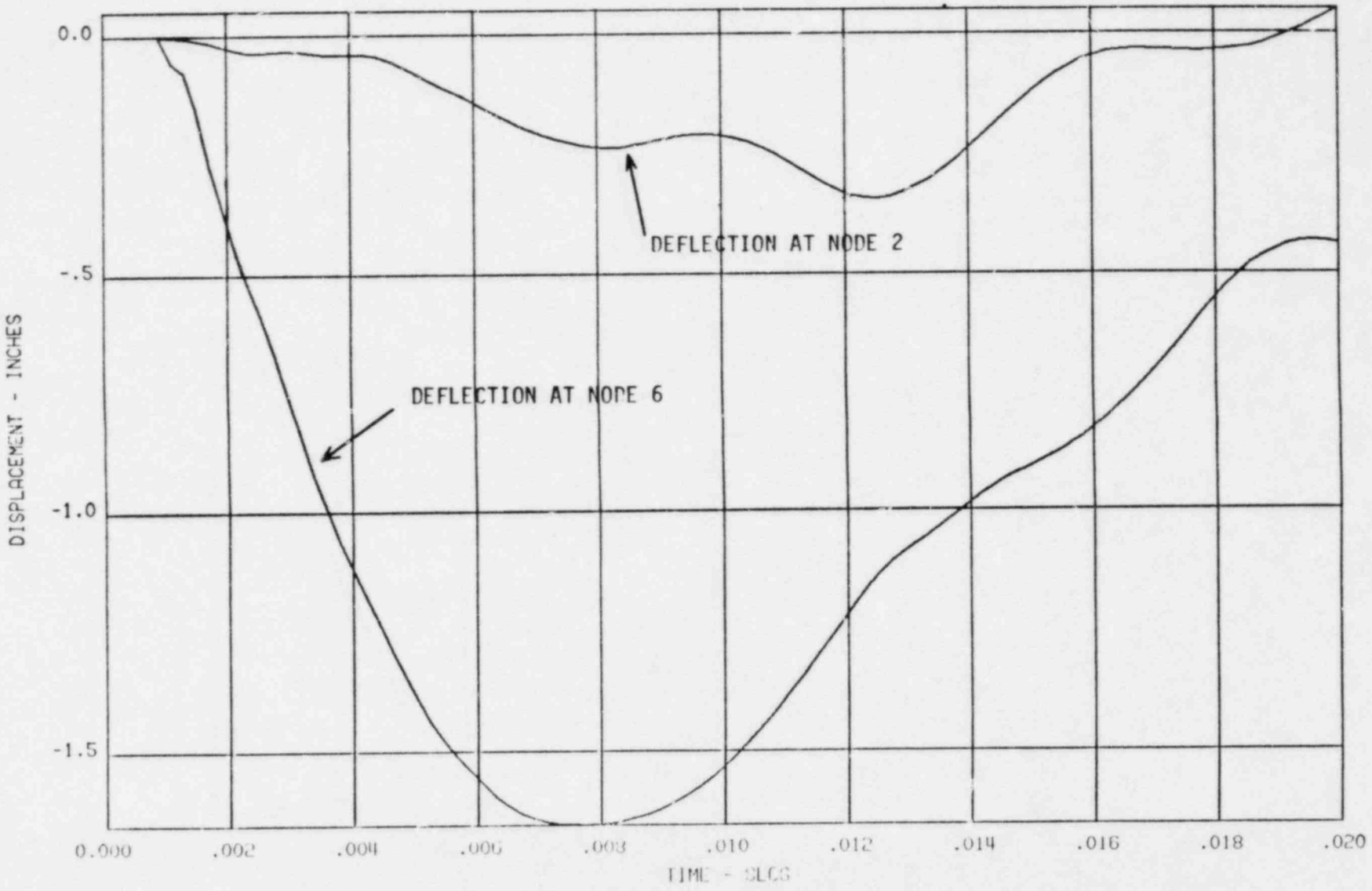

FIGURE 5 DISPLACEMENT AT NODES 2 AND 6

2.3 Energy Absorbed in Vessel Flange Region

Due to local yielding in the vessel flange region, not all of the energy transferred by the impact of the vessel head with the vessel will be transmitted into the remainder of the vessel. The energy dissipated at the point of impact can be determined by taking into account the plastic strain produced during the loading. The energy dissipated is given by:

$$U_d = \int_{\text{element 5}} \sigma_y \, d\epsilon \text{ (Volume)}$$

This may be approximated by:

$$U_d = \sigma_y \text{ (Volume of element 5) } \epsilon_{eff}$$

Where ϵ_{eff} is the average Von Mises effective plastic strain for element 5 when the maximum deflection of the impact node occurs. Substituting in the appropriate values from the finite element analysis give:

$$U_d = 70000 \ (42801.79)(.0072196)$$

$$U_d = 2.16 \times 10^7 \text{ in-lbf} = 1.8 \times 10^6 \text{ ft-lbf}$$

Thus the plastic yielding in the vessel flange region dissipates approximately 47% of the energy transferred due to impact of the vessel head and vessel.

3.0 SHROUD HEAD ASSEMBLY DROP

Dynamic response of the shroud and shroud support legs to an accidental drop of the shroud head assembly is found by a finite element analysis. The dropped shroud head is assumed to impact axisymetrically on the upper flange of the top guide shroud. As a result, the loads are transferred through the top guide shroud to the lower shroud, and subsequently to the vessel shell through the shroud support legs and attachment ring. The moments developed due to eccentricities in the load path are assumed to be carried by the top guide assembly and core support plate, where the eccentricities exist.

Figure 6 shows the model used in the finite element analysis. The model is axisymmetric using isoparametric quadrilateral elements. The core plate and top guide are simulated in the analysis by modifying the density of the elements respresenting them. The structure is fixed at the vessel attachments. Since the core plate is relatively stiff, the element representing it is not allowed to move radially. Two analyses were performed to determine the behavior of the shroud structure with and without the shroud support legs. In the first analysis an effective thickness was determined assuming the legs were fully circumferential. This results in a thickness of .44" along the length of the reinforcements, and .29" below the reinforcements. In the subsequent analysis the shroud support legs were not included in the finite element model to determine if the structural integrity of the shroud can be assured even without including the load carrying capability of the shroud support legs. This treatment of the shroud support legs is more applicable in the areas where no legs are present. The attachment ring is 1 inch instead of the actual 2 inches thick to compensate for the cutouts.

To simulate the drop, two gap elements are used as shown in Figure 6. The mass of the falling head is divided evenly between the two point masses shown.

The material behavior is taken to be perfectly plastic with a yield strength of 30 Ksi (Reference 4).

3.1 Velocity Of Shroud Head At Impact

The geometry and weight data for Peach Bottom 2/3 vessel and shroud head are as follows:

Vessel I. D. = 251.375" — Ref. 2

Shroud Head O. D. = 220" } GE Drawing 729E476

Weight = 139600 lbs }

As the shroud head drops through the vessel the downward motion is resisted by the pressure drop due to water flow through the annulus between the shroud head and the vessel inside diameter and by the flow through the standpipes. The terminal velocity that the shroud head attains is therefore dependent on the overall pressure drop. In this analysis, it is assumed that the shroud head has attained the steady state terminal velocity prior to impact.

Appendix B shows the calculation of an equivalent drag coefficient and the associated terminal velocity. In calculating the drag forces, it is assumed that the flow through the standpipe is negligible since the presence of the turning vane in the standpipes makes the flow tortuous. Also the effect of any small flow in the standpipes is more than made up by the pressure drop due to friction on the outside surface of the pipe. The following analysis demonstrates the calculation of the steady state terminal velocity.

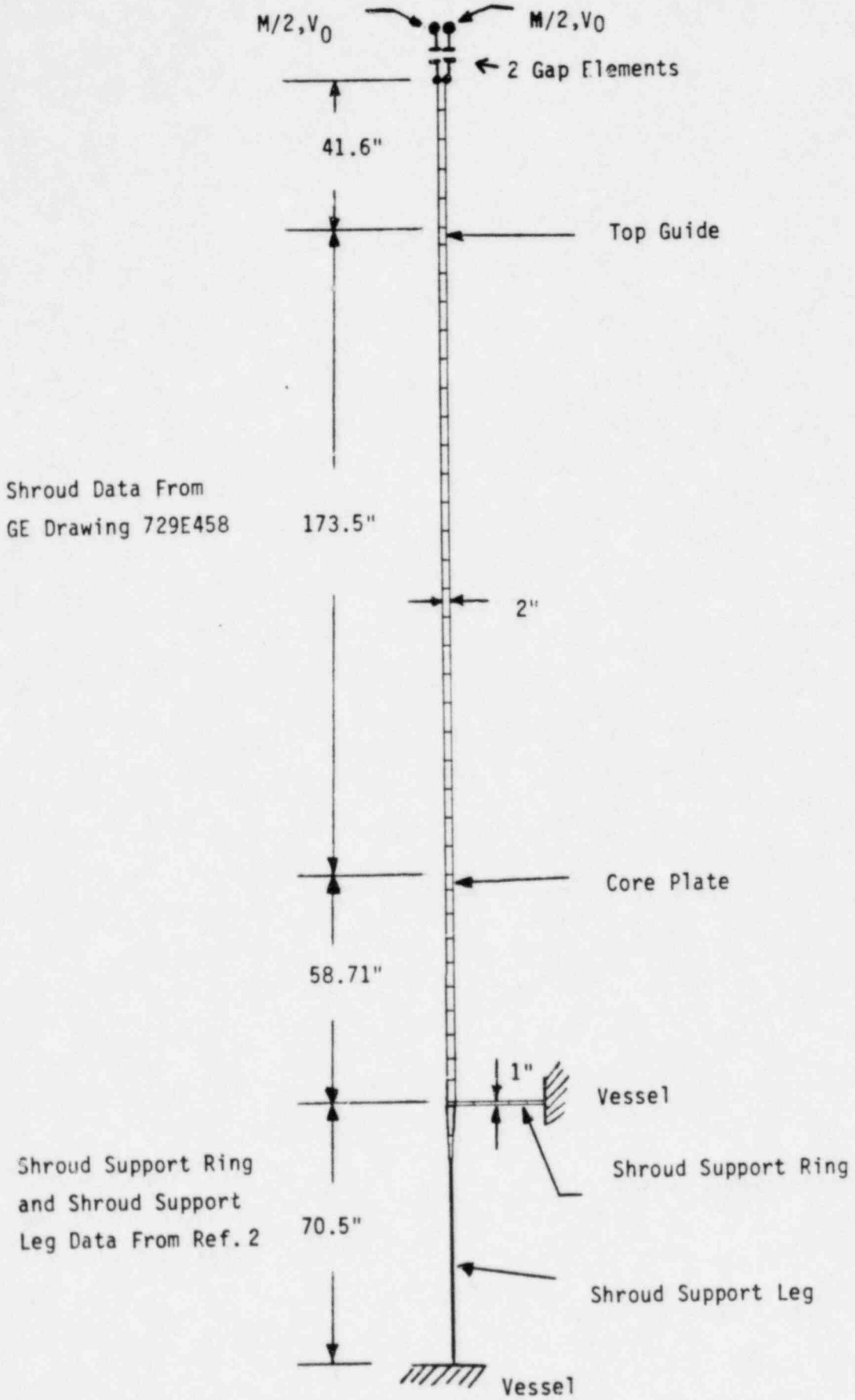

Figure 6 Shroud Head Drop Axisymmetric Finite Element Model

The shroud head projected area is:

$$A = \frac{\pi}{4} (220)^2 = 38013.3 \text{ in}^2$$

The vessel projected area is:

$$A_v = \frac{\pi}{4} (251.375)^2 = 49628.8 \text{in}^2$$

The annulus area is:

$$A_f = A_v - A = 49628.8 - 38013.3 = 11615.5 \text{ in}^2$$

The drag coefficient is given by (Appendix B):

$$C_d = \left[\frac{A_v}{CA_f} - 1 \right]^2$$

Where C = .8 for the geometry considered.

$$C_d = \left[\frac{49628.8}{.8(11615.5)} - 1 \right]^2 = 18.85$$

The steady state terminal velocity (derived in Appendix B) is:

$$V_t = \sqrt{\frac{2mg(1-\rho/b)}{A_v C_d}} \qquad \text{(Eq. 3-1.1)}$$

Where ρ = mass density of water = 9.36×10^{-5} lb/in^3

b = mass density of steel = 7.246×10^{-4} lb/in^3

Substituting into equation 3-1.1 gives:

$$V_t = \sqrt{\frac{2(139600)(1-\frac{.936}{7.246})}{9.36 \times 10^{-5} (49628.8)(18.85)}} = 52.9 \text{ in/sec}$$

3.2 Mass of Shroud Head

The mass of the falling shroud head is:

$$M = \frac{139600}{386.4} = 361.28 \text{ lbf sec}^2/\text{in}$$

Since the analysis is axisymmetric, the mass per radian is:

$$M = \frac{361.28}{2\pi} = 57.5 \text{ lbf sec}^2/\text{in-rad}$$

Half of this mass is applied at each gap element.

3.3 Shroud Head Drop Results

Results of the analysis indicate no inelastic behavior in the shroud. However yielding does occur in the shroud support legs. The yielding in the shroud support legs may be overly conservative due to the axisymmetric treatment of the legs. To determine if the shroud support legs were required for structural integrity of the shroud, an analysis was performed of the shroud head drop excluding the shroud support legs. The model used is shown in Figure 7. Results from the modified model analysis shows no inelastic behavior in the shroud or shroud support ring. Figure 8 shows the deflection at the point of impact and shroud - shroud support ring junction up to the time when peak deflections are reached. The maximum deflection at both locations is approximately .86 inches. The significance of this analysis is that the integrity of the shroud can be shown without taking credit for the load capability of the shroud support legs.

The main conclusion from the shroud head drop analyis is that the associated deformations are not excessive and that structural integrity and stability of the shroud are maintained. Thus no release of the coolant or radioactivity is expected.

4.0 STEAM DRYER ASSEMBLY DROP

An accidental drop of the steam dryer assembly is assumed to produce an impact on the shroud flange. The dryer assembly would first impact the steam dryer support brackets. It is conservatively assumed that these brackets do not impede the motion of the falling dryer assembly, the assembly would then impact upon the shroud head assembly. The impact would be absorbed by the same structure that would absorb the shroud head assembly drop. If it can be shown that the mass and kinetic energy of the steam dryer assembly are less than those of the shroud head, then no additional analysis is required since the conclusions from the shroud head drop analysis apply to the steam dryer assembly drop.

The weight of the steam dryer assembly is 45 tons which is less than the weight of the shroud head assembly. (Ref. GE Drawing # 731E711)

To determine if the kinetic energy of the steam dryer is less than the shroud head upon impact, the velocities may be compared.

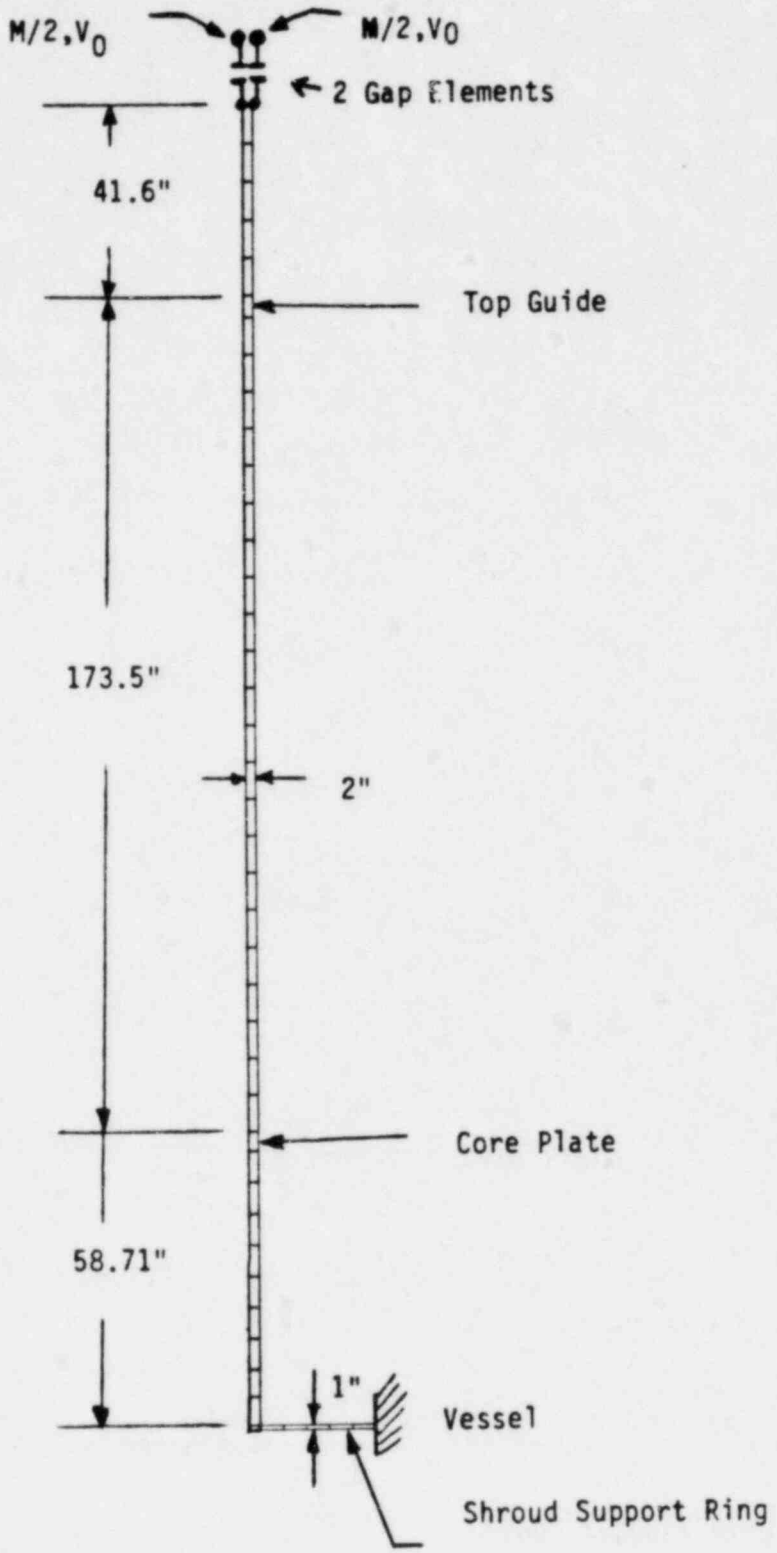

VESSEL

Figure 7 Shroud Head Drop Axisymmetric Finite Element Model

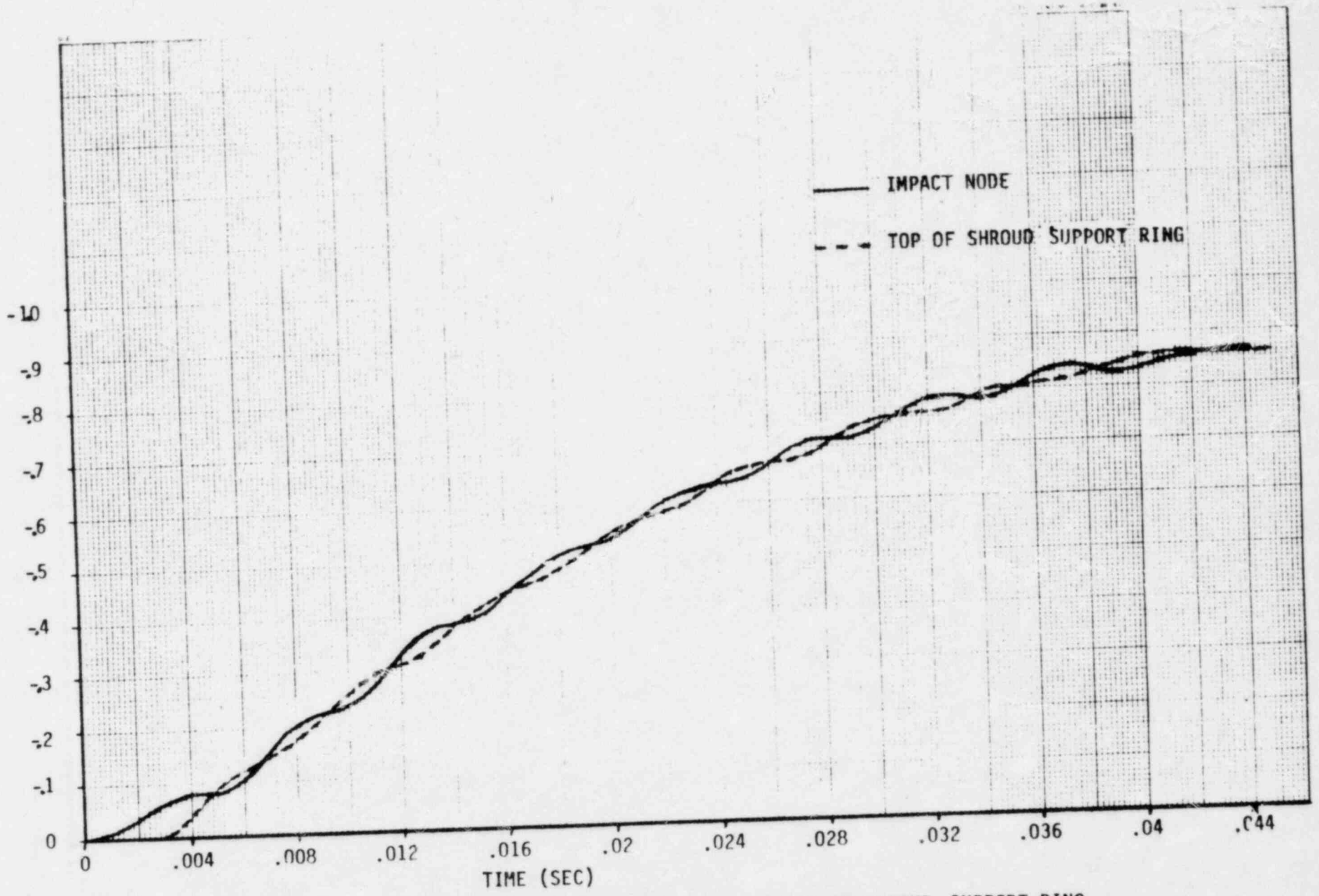

FIGURE 8 DEFLECTION AT IMPACT NODE AND TOP OF SHROUD SUPPORT RING

Using the same equation as for the velocity of the shroud head assembly (Eq 3-1.1) .

$$V_t = \sqrt{\frac{2mg(1-\frac{\rho}{\delta})}{\rho A_v C_d}} = 42.3 \text{ in/sec}$$

This is less than 52.7 in/sec which is the terminal velocity for the shroud head assembly.

Therefore since the mass and velocity of the steam dryer assembly is less than that of the shroud head assembly, the conclusions from the shroud head assembly drop analysis apply to the steam dryer assembly drop.

5.0 CONCLUSION

A detailed finite element elastic-plastic analysis was performed to evaluate the effects of the vessel head drop, shroud head drop and steam dryer assembly drop for the Peach Bottom 2/3 plants.

Structural integrity of the vessel and shroud is maintained even though some local yielding occurs following impact. Specifically, yielding occurs in the vessel flange to vessel junction area following vessel head drop and in the shroud support legs following the shroud head drop.

No damage to the fuel is predicted since the component geometry precludes direct impact on the fuel. In view of the fact that there is no significant damage to the reactor components or the fuel, no release of radioactivity is expected as a result of the drop.

REFERENCES

1. ANSYS Engineering Analysis System, Swanson Systems, Inc., March 1975

2. Final Design Document For General Electric - NED Peach Bottom III General Electric Order No. 205-B1156, Babcock & Wilcox Contract No. 610-0146-51 Vol. 1

3. General Electric Engineering Work Authorization No. EAF 93-CM
   Issued June 7, 1982

4. ASME Boiler And Pressure Vessel Code, Section III, Sub-section NA, 1980 Ed.

Appendix A - Stability Analysis of Skirt

A-1 Introduction

The result of the impact study of Section 2 indicates high stress and plastic deformation in the skirt. This observation raises the concern about the stability of the skirt under the impact load. To overcome this concern, the result of the impact study is examined herein to determine the cause of the high stress in the skirt. It is concluded that the high stress in the skirt is mainly due to simplifications of the structural model at the top and bottom of the skirt. These simplifications, which are acceptable in determining the gross structural response of the vessel, unfortunately induce unrealistic dynamic stress concentration in the skirt. Specifically, the simplifications are: (i) at the top of the skirt the downward branch of the vessel is not modelled (ii) at the bottom of the skirt the concrete foundation is modelled as an infinitely rigid and fixed body. These simplifications cause the stress wave generated by the impact to be "trapped" in the skirt and the stress in the skirt to be much higher than actual stress. A stress wave analysis described later in this section shows that the actual stress level in the skirt is probably as low as 50 to 60% of the value given by the impact analysis. Based on this result, the skirt is shown not to buckle under the impact load. Details of the stress wave and the buckling analysis are described in the remainder of this section.

A-2 Stress Wave Analysis

Figure A-1 shows the axial stresses obtained in the impact study for locations in the vessel and the skirt, respectively. In the figure, the times for the stress wave generated by the impact to travel from the vessel top to the top and bottom of the skirt are also given. The times are calculated using the elastic wave speed in a slender rod, c_o, which is an approximation of the actual wave speed in the vessel wall. These time values indicate that the rise and fall of stresses at various locations of the vessel and skirt are strongly related to wave propagation. For example, the result shows that the compressive axial stress at the vessel top is released when the reflected stress wave peak reaches the vessel top, and that the stress in the skirt starts to rise when the wave front reaches its top. Accordingly, the causes for the high stress level in the skirt should be identifiable by studying the wave propagation between the vessel and the skirt.

Reviewing the structural model for the impact study in light of wave propagation, one can immediately identify two possible explanations for the high stress level in the skirt. First, at the top of the skirt the lower portion of the vessel is not included in the structural model. Thus, the entire wave energy is channelled into the skirt to cause high stress. Secondly, at the bottom of the skirt, the boundary is assumed to be infinitely rigid in the structural model. Consequently, a compressional wave will be reflected as a compressional wave of the same amplitude, and the reflected wave will then be added to the incoming wave

to double the stress level. If these conservative approximations had not been used in the structural model, the stress level obtained for the skirt would have been much less than the value given by the impact analysis. To provide a quantitative estimate of the conservatism of the predicted stress level in the skirt, a simple analysis of the transmission and reflection of stress wave at the top and bottom of the skirt is presented herein. A detailed finite element wave analysis of the skirt is also conducted to confirm the results of the simple analysis.

The reflection and transmission of waves at a structural interface occur when the wave impedance of the joining structures are different. At the top of the skirt, the impedance of the vessel and skirt are different because there is a change in cross-sectional area. At the bottom of the skirt, a difference exists due to both changes of area and material properties. A stress wave passing through these interfaces can be partly transmitted and partly reflected. The amplitudes of the transmitted and reflected waves are dependent on the wave impedance (product of the density and the wave speed = ρc) on both sides of the interface. Considering the simplified case of the interface of two slender bars of different cross-sectional areas and materials (Figure A-2), the stress amplitude of the transmitted wave, σ_T and the reflected wave, σ_R can be related to the amplitude of the incident wave, σ_I. By equating the normal forces and velocities on both sides of the interface, the following relations are obtained.:

$$\sigma_T = \frac{2\,(\rho_2 c_2 / \rho_1 c_1)}{1 + (A_2/A_1)(\rho_2 c_2/\rho_1 c_1)}\,\sigma_I \qquad \text{(A-1a)}$$

$$\sigma_R = \frac{-1 + (A_2/A_1)(\rho_2 c_2/\rho_1 c_1)}{1 + (A_2/A_1)(\rho_2 c_2/\rho_1 c_1)}\,\sigma_I \qquad \text{(A-1b)}$$

where the subscripts 1 and 2 denote properties on the incident wave and transmitted wave sides of the interface, respecitvely; ρ is the mass density and c the elastic wave speed of the materials; A is the cross-sectional areas of the joining structural components. These equations can be used as approximate formulas to estimate the stress level in the skirt due to stress wave propagation.

In the structural model for impact study, since the lower portion of the vessel is omitted at the top of the skirt, the wave propagation only occurs between the skirt and the upper portion of the vessel (Figure A-3). Using Equations (A-1a) and (A-1b), and setting $\rho_1 c_1 = \rho_2 c_2$, $A_2/A_1 = 0.204$, where the subscripts 1 and 2 denote properties of the upper portion of the vessel and of the skirt, respectively, the stress level in the skirt due

to stress wave propagation can be shown to be 4.88 times of that of the vessel when the stress wave propagates from the vessel into the skirt. At the bottom of the skirt, since the support is modelled as rigid; i.e., $\rho c = \infty$, Equation (A-1b) shows that a stress wave in the skirt will be reflected unchanged at the rigid support. Thus the stress level in the skirt will be twice the amplitude of the incident stress wave. Taking into consideration the effects of both the vessel skirt interface and the rigid support, one can expect stress level in the skirt to be approximately 10 (2x4.88) times that of the vessel. This rough estimate appears to agree with the results of the impact study shown in Figure A-1, i.e., the stress of finite element 1 (representing the skirt) is about 8 times of the stress in element 2 (representing the vessel location immediately above the vessel).

The above estimate of stress in the skirt is drastically reduced, if the presence of the lower portion of the vessel and of the flexibility of the skirt support is included. In this case, an incident wave from the upper part of the vessel will be transmitted into not only the skirt but also the lower part of the vessel (Figure A-3). Similar calculations can be carried out as before, using $A_T = A_{Lv} + A_S$ in Equation (A-1a) and (A-1b), where the subscript Lv denotes area value of the lower vessel and S the area of the skirt. The new calculations show that the stress level in the skirt is only 0.83 times the stress in the upper vessel. This value is substantially lower than the 4.88 obtained for the case of omitted lower vessel. Similar reduction of stress level can be shown at the skirt support if the support is assumed to be non-rigid. Assuming the support to be made of concrete (mass density = 2.25×10^{-4} lb-sec^2/in^4 and Young's modulus = 3.33×10^6 psi) and ignoring the effect of area change, Equation (A-1b) shows that the reflected wave due to an incident compressional wave in the skirt is a tensile wave whose amplitude is 0.92 times of that of the incident wave. Accordingly, in the actual structure, the dynamic stress in the skirt will probably be quickly released rather than be amplified by the reflected wave as shown earlier for the rigid support model. Before unloading, the stress level in the skirt would be about the same as in the vessel.

To confirm the foregoing observations concerning the significant effects of the presence of lower vessel and support flexibility on the dynamic stress in the skirt, a special finite element dynamic analysis of the skirt is carried out. The finite element model used in this analysis is given in Figure A-4. It is a detailed model of the skirt and its surrounding structures; it includes the entire skirt, a portion of the concrete support and a portion of the upper and lower vessel located near the top of the skirt. With negligible effects on the usefulness of the results, the model is taken to be a plane strain model with thickness of unity. The model is supported at its boundary nodes by springs and dampers in the global x and y directions. Sufficient damping is assigned to the dampers to absorb all the incident wave energy at the model boundary, so that the analysis results will not be affected by reflected waves from the boundary. The model initially at rest is subjected to a suddenly applied constant pressure pulse at the upper end of the vessel.

In general agreement with the results of the foregoing wave study, the finite element results show that the maximum stress in the skirt is only 1.3 times of the stress in the vessel. Moreover, the dynamic stress in the skirt is quickly released although it takes more than a few traverses of the stress wave in the skirt to accomplish it.

From the foregoing results, one can conclude that to determine the stress in the skirt, it is essential to include in the model the lower portion of the vessel and the flexibility of the skirt support. The results also show that the maximum magnitude of the actual stress in the skirt is about the same as that of the vessel. Accordingly, for the buckling analysis, we can use as the skirt stress the average of the stresses obtained in the impact study for the vessel and the skirt; i.e., stresses in Elements 2 and 1 in the finite element model for the impact study. The maximum skirt stress obtained in this way is about 45 ksi (see Figure 1). This stress value is instead used in the buckling analysis of the skirt.

A-3 Vessel Support Skirt Buckling Analysis

A conservative elastic-plastic buckling analysis is performed to evaluate the stability of the skirt under the impact loading following the head drop. The dynamic stress in the skirt is assumed to be uniform around the circumference of the skirt, and the stress is applied statically. Since the inertia of the material tends to help prevent buckling at the beginning stage, it is conservative to ignore the inertia in the estimate of buckling load. Some experimental data have been published in the literature showing that cylinders buckle at higher stresses under dynamic than static loads.

To determine the buckling stress, it is necessary to first identify the governing mechanisms. Past research has shown that two geometric parameters are particularly helpful in determining the buckling load of circular cylinder under axial load; i.e., r/t and $(1-\nu^2)^{\frac{1}{2}}L^2/rt$, where r is the radius, t is the thickness, and L is the length (or height) of the cyclinder; ν is the Poisson's ratio of the material. For the skirt r/t = 91 and $Z_L = (1-\nu^2)^{\frac{1}{2}}L^2/rt = 32.7$. The r/t value indicates that the skirt is a moderately thick cylinder whose buckling stress is not very sensitive to randomly-distributed geometric imperfections, if it buckles at stress above the proportional limit where the material ceases to be linear elastic. The value Z_L of the skirt shows that it is an "intermediate-length" cylinder whose buckling stress and deformation are strongly affected by the length and end condition of the cylinder. An analytical prediction of the buckling stress is difficult. Gerard provided a conservative empirical formula for the prediction of the buckling stress for cylinders with clamped ends (Reference A-1).

$$\sigma_{cr} = \frac{k_c \pi^2 E t^2}{12 (1-\nu^2) L^2} \qquad \text{(A-2a)}$$

$$k_c = k_p + (0.581\, C\, z_L)^2 / k_p \qquad \text{(A-2b)}$$

where k_c is the buckling coefficient for a flat plate and C is a function of r/t. For r/t = 91, C = 0.43, and k_p = 4.0. Substituting appropriate values in (A-2a) and A-2b), the elastic buckling stress of the skirt is obtained to be 158 ksi. Since this value exceeds the yield stress of the material (assumed to be 60 ksi for this analysis), the skirt will buckle plastically. To find the buckling stress, a plasticity-reduction factor of η can be used; i.e.,

$$(\sigma_{cr})_{pl} = \eta\, (\sigma_{cr})_{el} \qquad \text{(A-3)}$$

where the subscripts pl and el denotes elastic and plastic buckling stresses, and the elastic buckling stress is obtained using Equation (A-2a). The formula for η of a flat plate is used herein, since for this case it gives a slightly more conservative result than the formula for a long cylinder. For a flat plate,

$$\eta = \frac{1-\nu^2}{1-\mu^2}\left(\frac{1}{4}\frac{E_s}{E} + \frac{3}{4}\frac{E_t}{E}\right) \qquad \text{(A-4)}$$

where $\mu = 1/2 - (1/2 - \nu)E_s/E$; ν and E are Poisson's ratio and Young's modulus of the skirt material, respectively; $E_s = \sigma/\varepsilon$ is the secant modulus and $E_t = d\sigma/d\varepsilon$ is the tangent modulus of the stress-strain curve of the material. The E_s and E_t corresponding to the buckling stress can be conveniently evaluated using the Ramberg-Osgood representation of the stress-strain curve of the skirt material (Figure A-6):

$$\frac{E\varepsilon}{\sigma_o} = \frac{\sigma}{\sigma_o} + 1.12\left(\frac{\sigma}{\sigma_o}\right)^{9.71} \qquad \text{(A-5)}$$

where σ_o = 60 ksi, and E = 30×10^3 ksi.

By trial and error, the plastic buckling stress of the skirt under symmetric axial load can be obtained as 54 ksi. This value is greater than 45 ksi which was determined in the foregoing stress wave analysis to be the maximum dynamic stress generated in the skirt by the shroud head impact. Consequently, the skirt will be able to withstand the impact load without buckling.

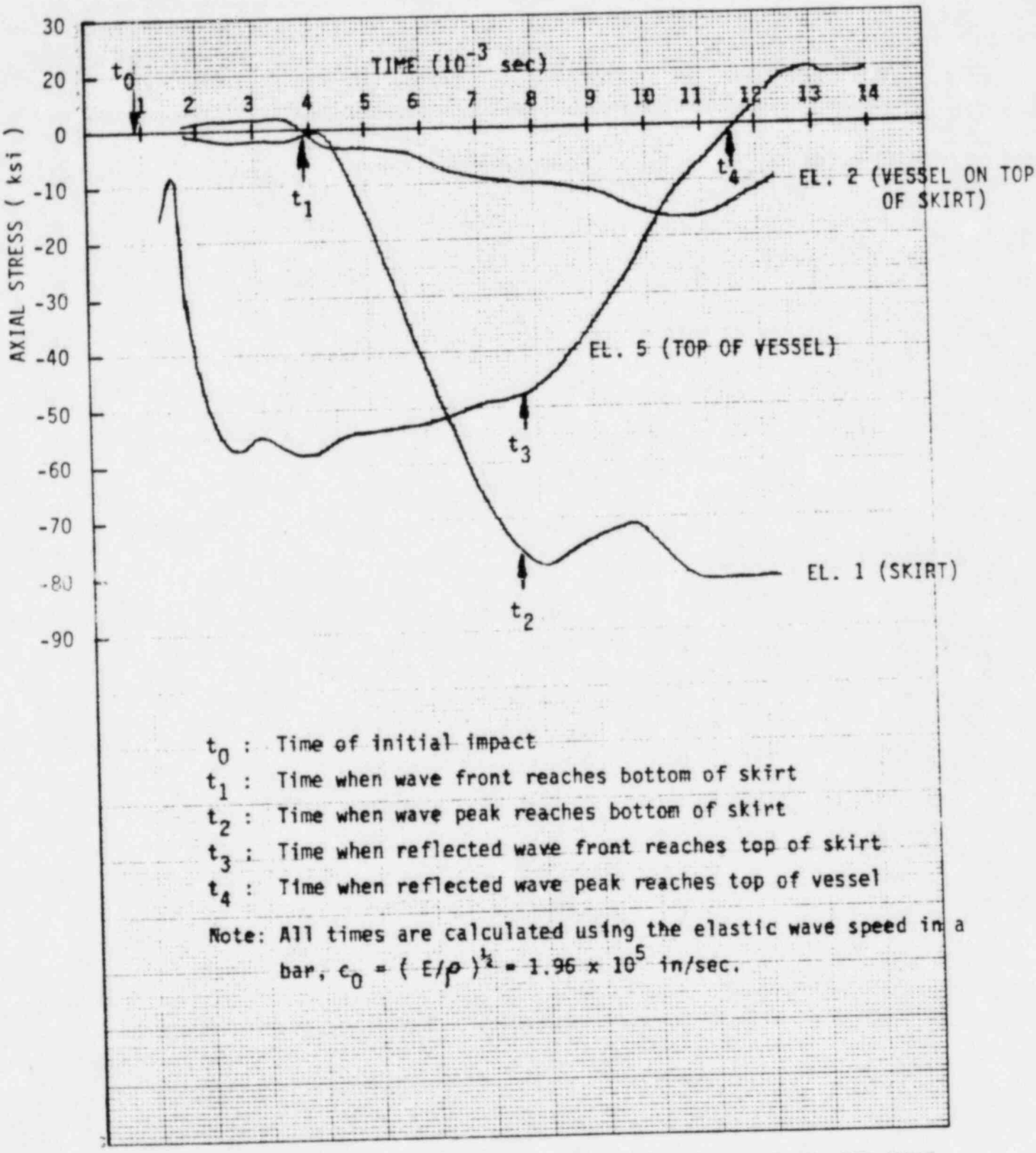

t_0 : Time of initial impact

t_1 : Time when wave front reaches bottom of skirt

t_2 : Time when wave peak reaches bottom of skirt

t_3 : Time when reflected wave front reaches top of skirt

t_4 : Time when reflected wave peak reaches top of vessel

Note: All times are calculated using the elastic wave speed in a bar, $c_0 = (E/\rho)^{\frac{1}{2}} = 1.96 \times 10^5$ in/sec.

FIGURE A-1 CORRELATION OF AXIAL STRESSES FROM IMPACT STUDY WITH WAVE PROPAGATION PHENOMENA

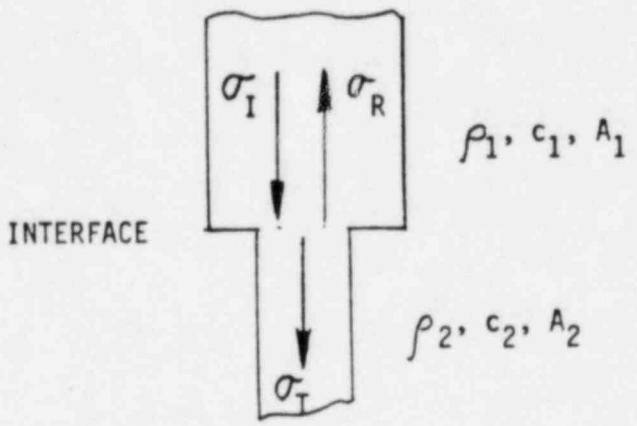

FIGURE A-2 WAVE PROPAGATION ACROSS A STRUCTURAL INTERFACE

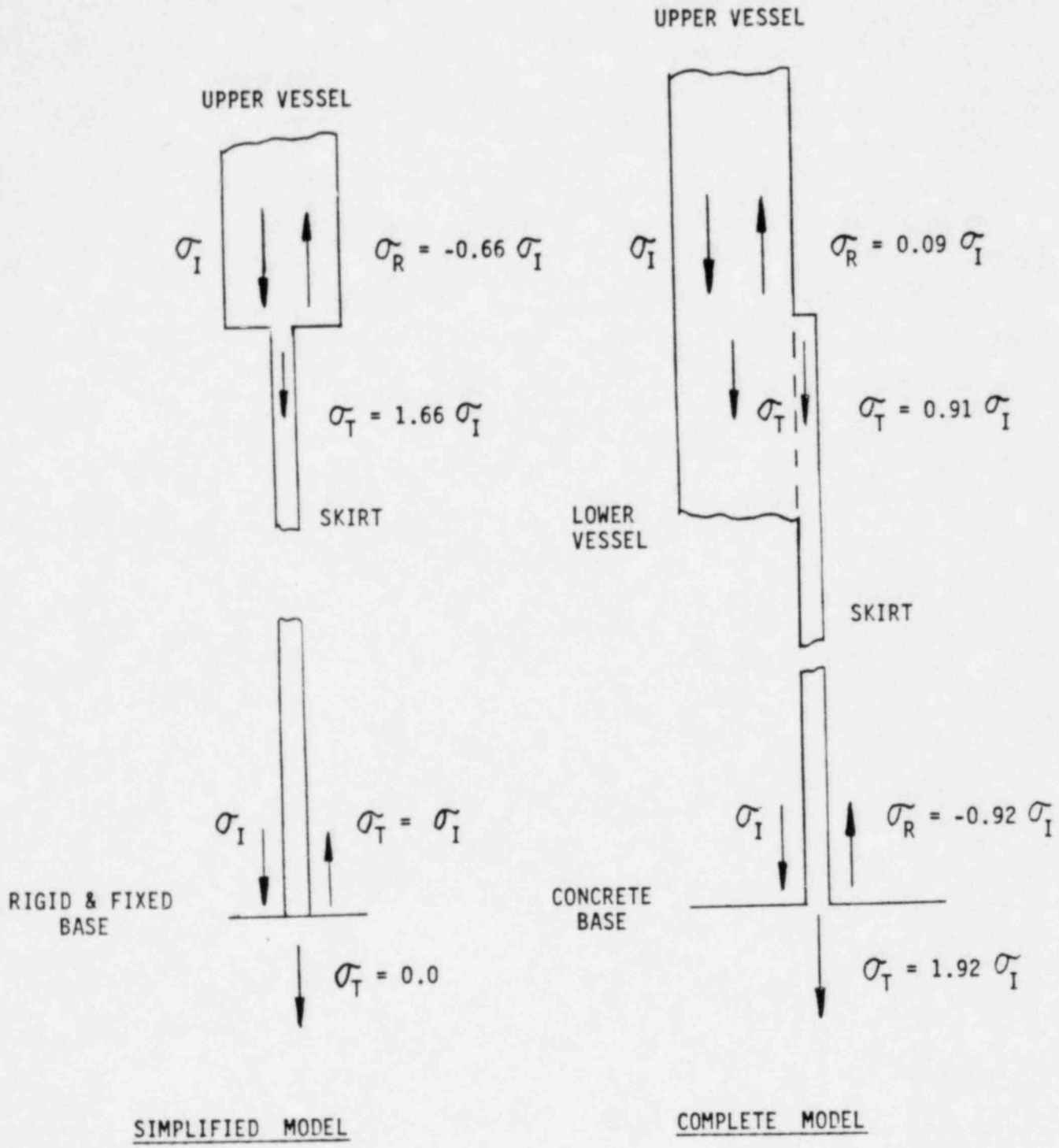

FIGURE A-3 SCHEMATIC OF SIMPLIFIED AND COMPLETE SKIRT MODELS FOR WAVE PROPAGATION STUDY

FIRURE A-4 FINITE ELEMENT MODEL FOR WAVE PROPAGATION STUDY

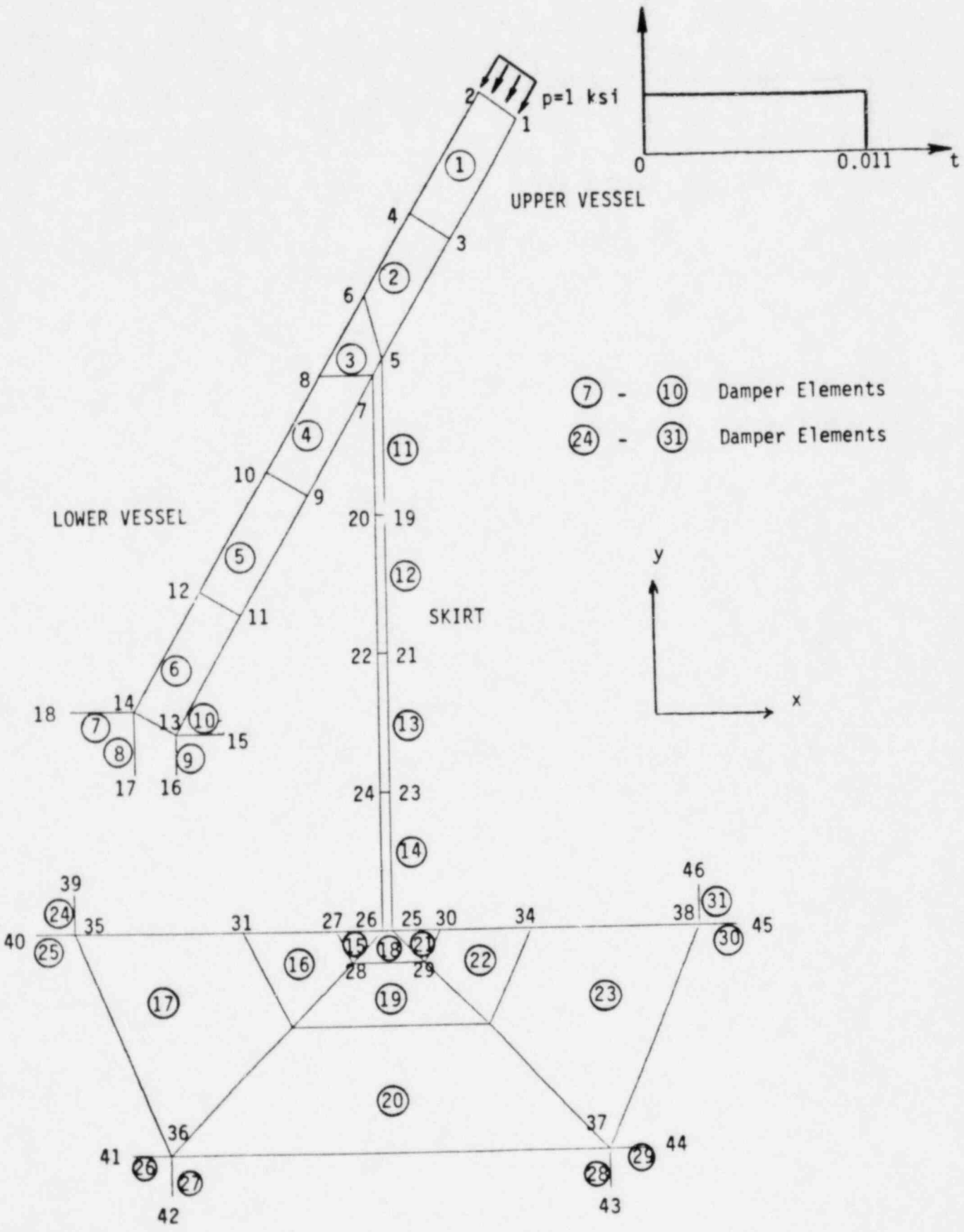

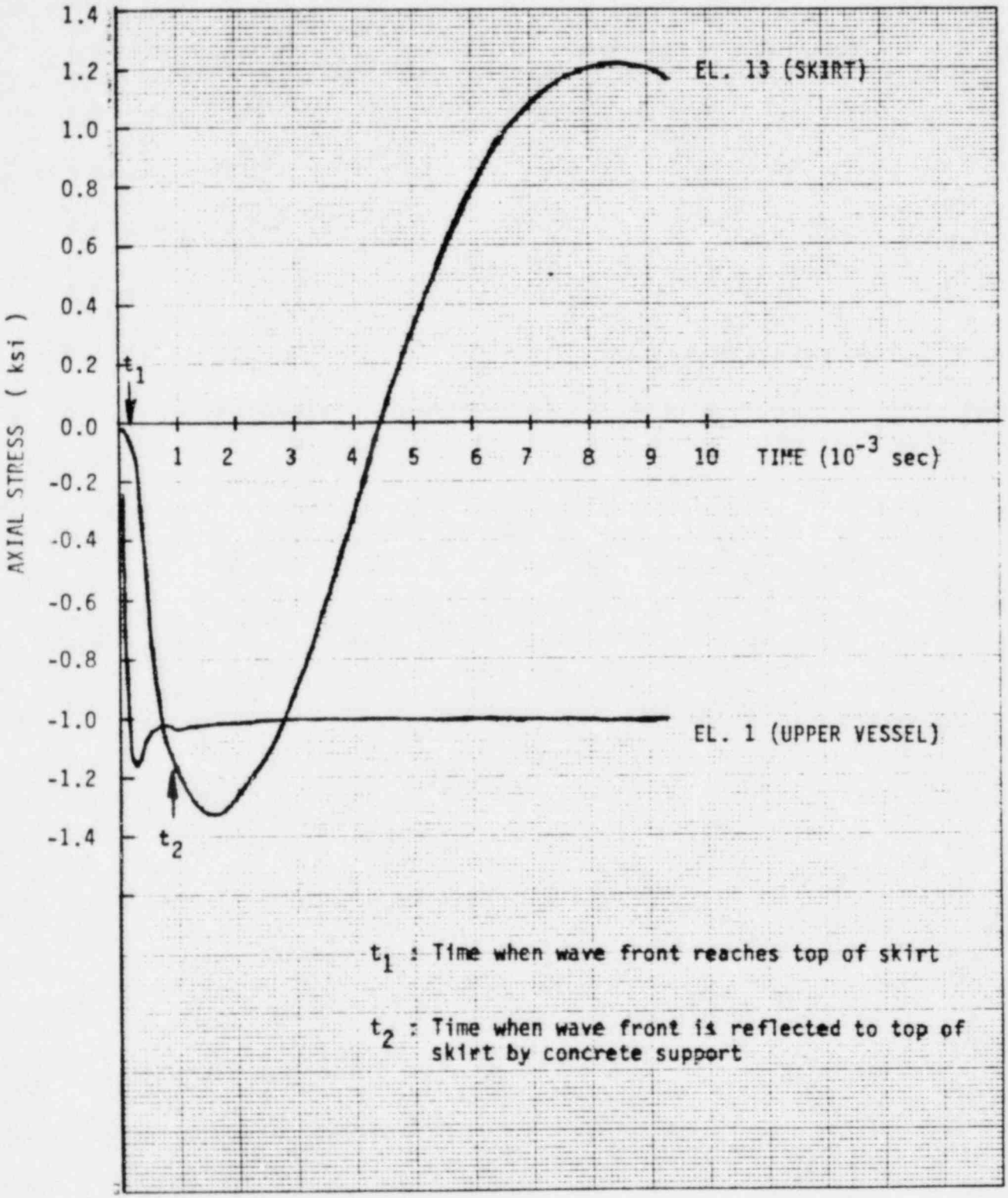

FIGURE A-5 AXIAL STRESS IN SKIRT DUE TO WAVE PROPAGATION

(FINITE ELEMENT MODEL IN FIGURE A-4)

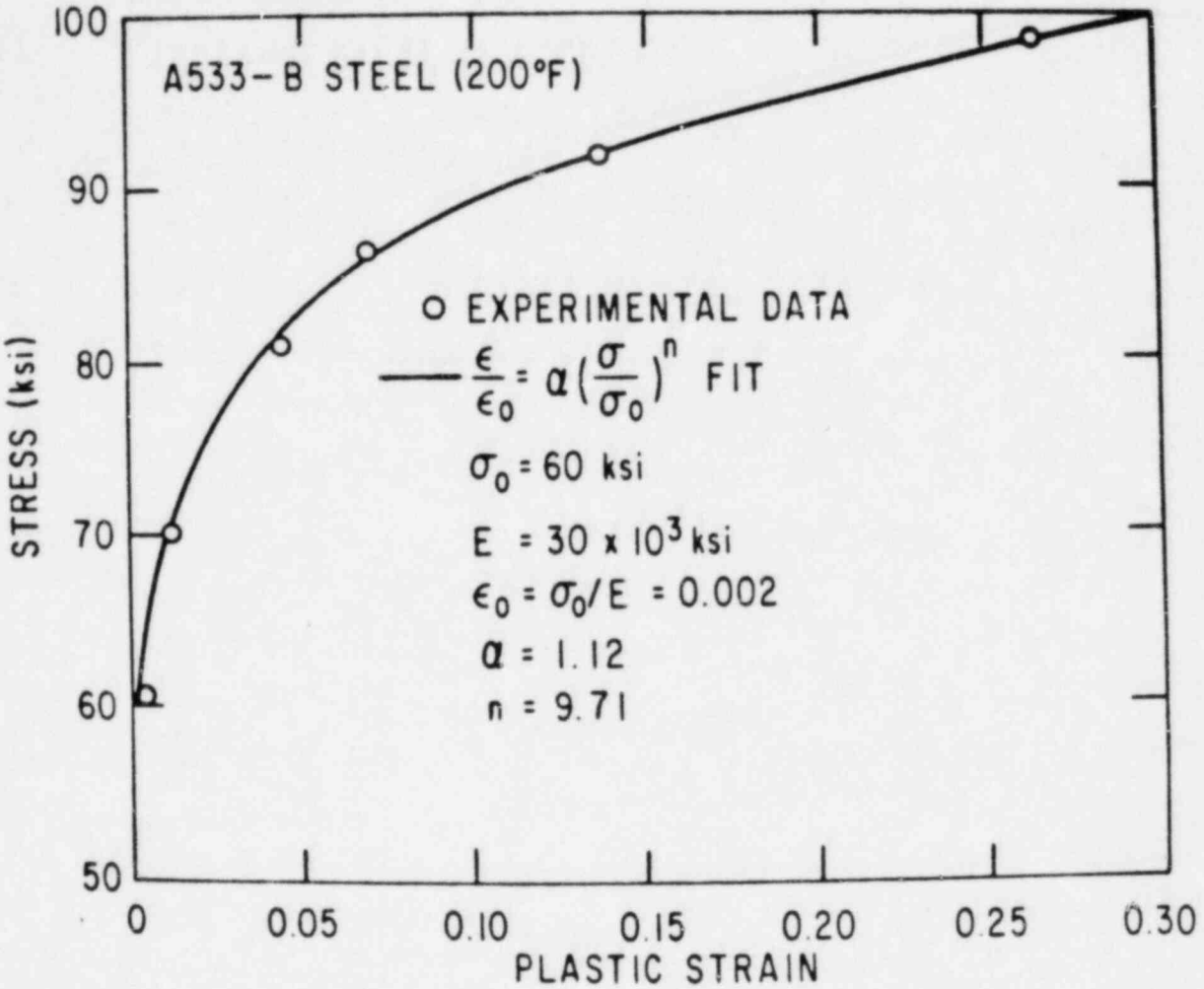

Figure A-6. Stress-strain curve for A533B steel at 200°F and its representation by the Ramberg-Osgood law.

Reference

A-1 Gerard, G., and Becker, H., "Handbook of Structural Stability, Part III - Buckling of Curved Plates and Shells," NACA TN 3783, August 1957.

APPENDIX B

SHROUD HEAD VELOCITY UNDER SUBMERGED CONDITIONS

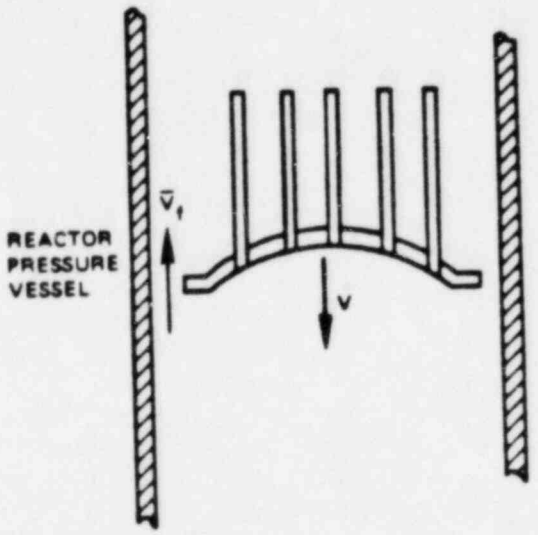

Figure B-1. Schematic of Shroud Head Drop

Define:

V	=	shroud head velocity
m	=	shroud head mass
A	=	projected area of the shroud head normal to V
V_f	=	flow velocity relative to the shroud head (neglect friction and assume that velocity through the steam separators is negligible).
A_f	=	total flow area = $A_v - A$
A_v	=	vessel cross-section area
ρ	=	mass density of water
δ	=	mass density of steel
S	=	displacement coordinate with S = 0 when V = 0
C_D	=	drag coefficient in equation drag force = $C_D \cdot \rho \cdot \frac{V^2}{2} \cdot$ area

o CALCULATION OF THE DRAG COEFFICIENT C_D AND THE DRAG FORCE

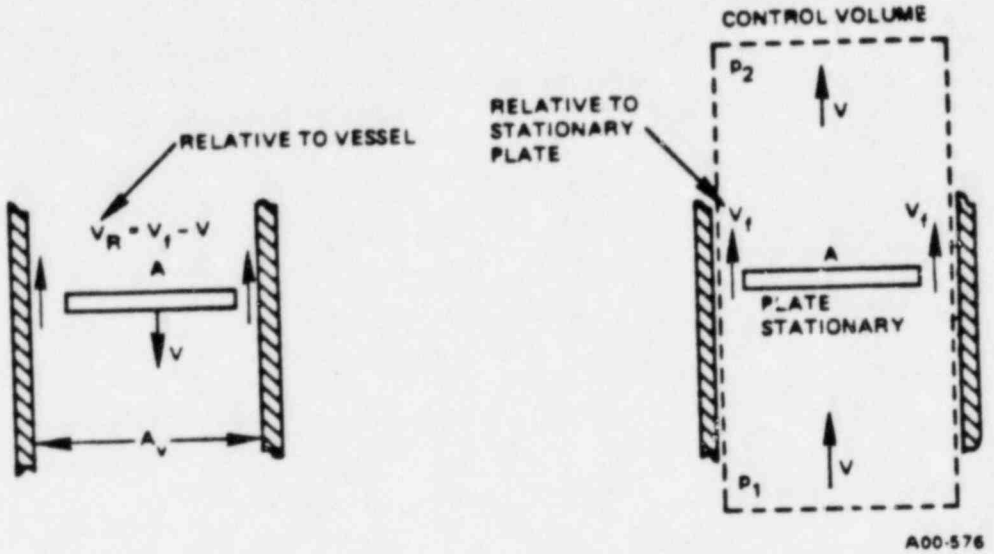

Figure B-2. Relative Velocities in the Shroud Head Drop

The actual situation is shown in the figure above on the left hand side. A plate with projected area A (representing the shroud head) moves downwards with velocity V. Shown on the right hand side above is the same system with the plate made stationary by adding a velocity component V, to the vessel. Now, consider a control volume of the fluid as shown by the dotted line. At the bottom, the pressure is P_1 and the velocity V. For the time being, neglect gravitational considerations. The fluid passes through the annular area, A_f, with velocity V_f. At some distance, the velocity V is regained, but due to enlargement of area, there is some head loss. Therefore, the pressure is only P_2 at the upper end of the control volume.

The head loss due to the enlargement of the cross-sectional area to A_v is

$$h_L = \frac{(V_f - V)^2}{2g} \qquad \text{(Equation B-1)}$$

The velocity V_f is at the vena contracta.

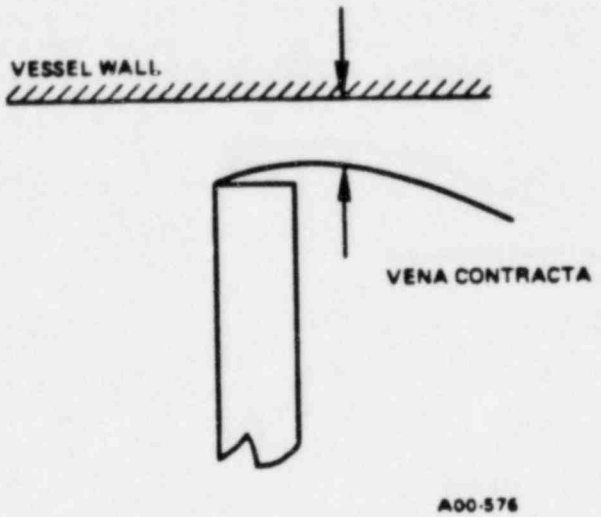

Figure B-3. Vena Contracta for Fluid Flow

The cross-sectional area at the vena contracta is $C_c \cdot A_f$, where C_c is the coefficient of contraction. Values of C_c in the literature range from 0.5 to 1.0. For ideal flow through a rectangular sharp edged orifice classical hydrodynamics yields a value of 0.61.

Figure B-4 shows $C_c \cdot C_v$ for orifices with diameter ratios D_1/D_o. Since C_v is very close to 1.0, the value of $C_d \sim C_c \cdot D_0/D_1$ in our case (i.e., A/A_v) may vary from 0.8 to 0.9. Based on this, a conservative value of 0.8 is selected for C_c. This value is considered to be reasonable since Reference B1 assumes a value of 0.66 for C_c in the case of flow past an obstruction in a pipe. Note that it is conservative to use as large a value of C_c as is reasonable:

$$V_f = \left(\frac{A_v}{CA_f}\right) V \qquad C = C_v$$

$$h_L = \frac{V^2}{2g}\left[\frac{A_v}{CA_f} - 1\right]^2 \qquad \text{(Equation B-2)}$$

*Hydraulics and Fluid Mechanics by E. H. Lewitt, Publisher, Sir Isaac Pitman, London, 1958 edition, p. 112.

now

$$P_1 - P_2 = \rho h_L = \rho \frac{V^2}{2g} \cdot \left[\frac{A_v}{CA_f} - 1\right]^2 = \rho \frac{V^2}{2} \left[\frac{A_v}{CA_f} - 1\right]^2 \quad \text{(Equation B-3)}$$

This is now in mass density units rather than weight units.

The free body diagram of the control volume shows the net reaction force on the fluid = $(P_1 - P_2) \cdot A_v$. This force is equal to the drag force on the shroud head.

FROM: FLUID MECHANICS WITH ENGINEERING APPLICATIONS, BY DAUGHERTY AND FRANZINEI, McGRAW HILL, 1965, EDITION p 358

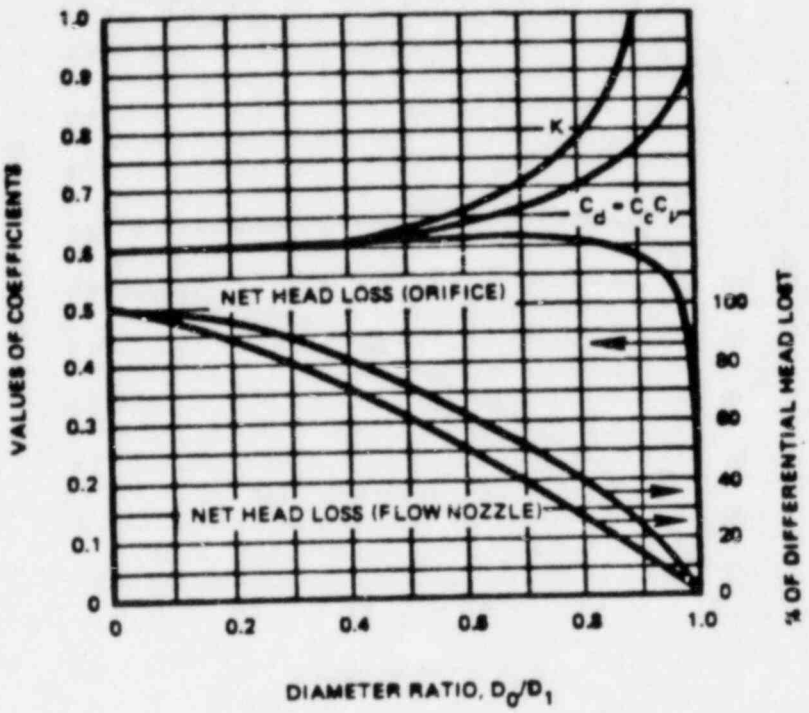

Figure B4. Coefficients for Sharp-Edged Orifice with Pressure Differential Measured Either at the Flanges or at the Vena Contracta. Also Head Loss Across Orifice and Flow Nozzle. All Curves are for $N_R (D_1 V_1 \rho_1 / \mu) > 10^6$.

From: FLUID MECHANICS With Engineering Applications, By Daugherty and Franzinei, McGRAW HILL, 1965, Edition p 358.

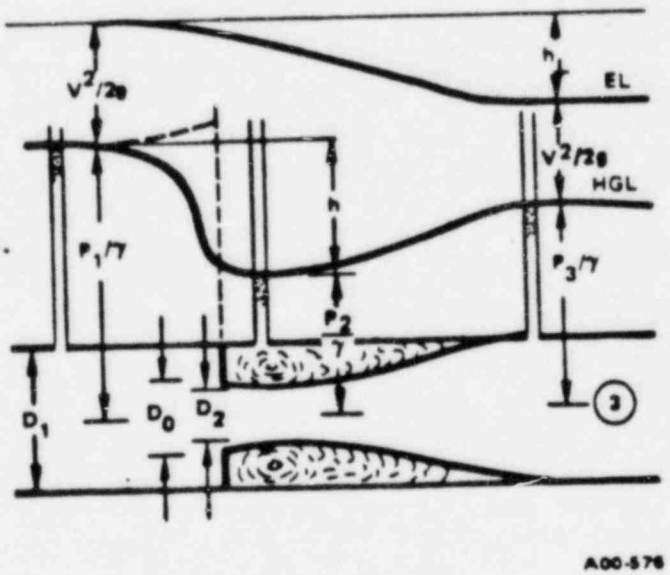

Figure B5. Thin-Plate Orifice in a Pipe

The Drag force $= \rho \cdot A_V \cdot \left[\frac{V^2}{2}\right] \cdot \left[\frac{A_V}{CA_f} - 1\right]^2$ (Equation B-5)

If the drag force is defined as $C_D \cdot \rho \cdot \left[\frac{V^2}{2}\right] \cdot A_V \cdot$ then:

$$C_D = \left[\frac{A_V}{CA_f} - 1\right]^2 \quad \text{(Equation B-6)}$$

o Determination of Velocity V:

The equation of motion is as follows:

$$F = m \dot{v} \quad \text{(Equation B-7)}$$

Two forces on the decending body are:

Buoyancy force $= mg\ (1 - \rho/\delta)$ (Equation B-8)

Drag force $= C_D \cdot \left[\frac{V^2}{2}\right] \cdot A_V \cdot \rho$ (Equation B-9)

Therefore we have:

$$mg\ (1 - \rho/\delta) - C_D \cdot \left[\frac{V^2}{2}\right] \cdot A_V \cdot \rho = m\dot{v} \quad \text{(Equation B-10)}$$

Since $\dot{v} = \frac{dv}{dt}$ and $V = \frac{ds}{dt}$

Then $dt = \frac{ds}{V}$ and $\dot{v} = V \frac{dv}{ds}$

Combining the above equations and solving for ds.

$$mg\ (1 - \rho/\delta) - C_D \cdot \rho \cdot \left[\frac{V^2}{2}\right] \cdot A_V = mV \cdot \left[\frac{dv}{ds}\right]$$

$$\text{or } ds = \frac{mV\ dv}{mg\ (1 - \rho/\delta) - C_D \cdot \rho \left[\frac{V^2}{2}\right] \cdot A_V}$$

$$\text{or } ds = \frac{(2mV/\rho\ C_D A_V)\ dv}{\frac{2mg}{\rho C_D A_V} \cdot (1 - \rho/\delta) - V^2} \qquad \text{(Equation B-11)}$$

$$\text{Define } a = \frac{2mg}{\rho \cdot C_D \cdot A_V} \cdot (1 - \rho/\delta)$$

Then,

$$\int_o^S ds = \frac{2m}{\rho C_D A_V} \int_o^V \frac{V\ dv}{a - V^2} \qquad \text{(Equation B-12)}$$

From standard integration formulas, we have

$$\int \frac{V\ dv}{a - V^2} = -\frac{1}{2} \ln (a - V^2) \qquad \text{(Equation B-13)}$$

$$S = -\frac{m}{\rho C_D A_V} \left[\ln (a - V^2) \right]_o^V$$

$$= -\frac{m}{\rho C_D A_V} \cdot \ln \left(1 - \frac{V^2}{a}\right) \qquad \text{(Equation B-14)}$$

Solving for V^2,

$$V^2 = a \left[1 - e^{-\rho A_V C_D\ S/m} \right] \qquad \text{(Equation B-15)}$$

An inspection of above equation shows that if the falling height, S through the liquid is large enough, then, the second term is essentially zero, therefore,

Terminal steady state velocity $V_t = \sqrt{a}$

$$= \sqrt{\frac{2mg\ (1 - \rho/\delta)}{\rho C_D A_V}} \qquad \text{(Equation B-16)}$$

Conversely, we can also determine height, S, through which a body has to fall before it essentially attains steady state terminal velocity. For example, let us determine the formula for drop height 'S' when shroud head attains 90% of steady state velocity.

$$0.9^2 = 1 - e^{-\rho A_V C_D S/m} \qquad \text{(Equation B-17)}$$

$$\text{or } \rho A_V C_D S/m = 1.66$$

$$S_{90} = \frac{1.66\ m}{\rho A_V C_D} \qquad \text{(Equation B-18)}$$

Also, given a drop height, we can find what percentage of steady state velocity it will reach at the end of this drop height.